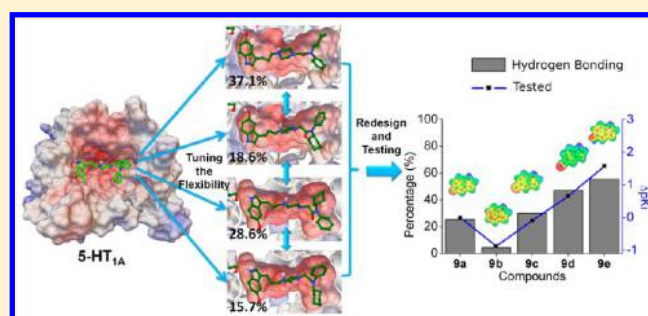


Higher-Affinity Agonists of 5-HT_{1A}R Discovered through Tuning the Binding-Site Flexibility

Peng Lian,^{†,§} LinLang Li,^{‡,§} Chuanrong Geng,[†] Xuechu Zhen,^{*,‡} and Wei Fu^{*,†}[†]Department of Medicinal Chemistry & Key Laboratory of Smart Drug Delivery, Ministry of Education, School of Pharmacy, Fudan University, Shanghai 201203, China[‡]Jiangsu Key Laboratory for Translational Research for Neuropsychiatric-Diseases, Department of Pharmacology, College of Pharmaceutical Sciences, Soochow University, Suzhou 215123, China

Supporting Information

ABSTRACT: Discovery of high-affinity and high-selectivity agonists of 5-HT_{1A}R has become very attractive due to their potential therapeutic effects on multiple 5-HT_{1A}R-related psychological and neurological problems. On the basis of our previously designed lead compound **FW01** ($K_i = 51.9$ nM, denoted as **9a** in the present study), we performed large-scale molecular dynamics simulations and molecular docking operations on 5-HT_{1A}R-**9a** binding. We found the flip-packing events for the headgroup of **9a**, and we also found that its tail group could bind flexibly at the agonist-binding site of 5-HT_{1A}R. By finely tuning the flip-packing phenomenon of the **9a** headgroup and tuning the binding flexibility of **9a** tail group, we virtually designed a series of new **9a** derivatives through molecular docking operations and first-principles calculations and predicted that these newly designed **9a** derivatives should be higher-affinity agonists of 5-HT_{1A}R. The computational predictions on the new **9a** derivatives have been confirmed by our wet-experimental studies as chemical synthesis, binding affinity assays, and agonistic-function assays. The consistency between our computational design and wet-experimental measurements has led to our discovery of higher-affinity agonists of 5-HT_{1A}R, with ~50-fold increase in receptor-binding affinity and ~25-fold improvements in agonistic function. In addition, our newly designed 5-HT_{1A}R agonists showed very high selectivity of 5-HT_{1A}R over subtype 5-HT_{2A}R and also over three subtypes of dopamine receptors (D₁, D₂, and D₃).



INTRODUCTION

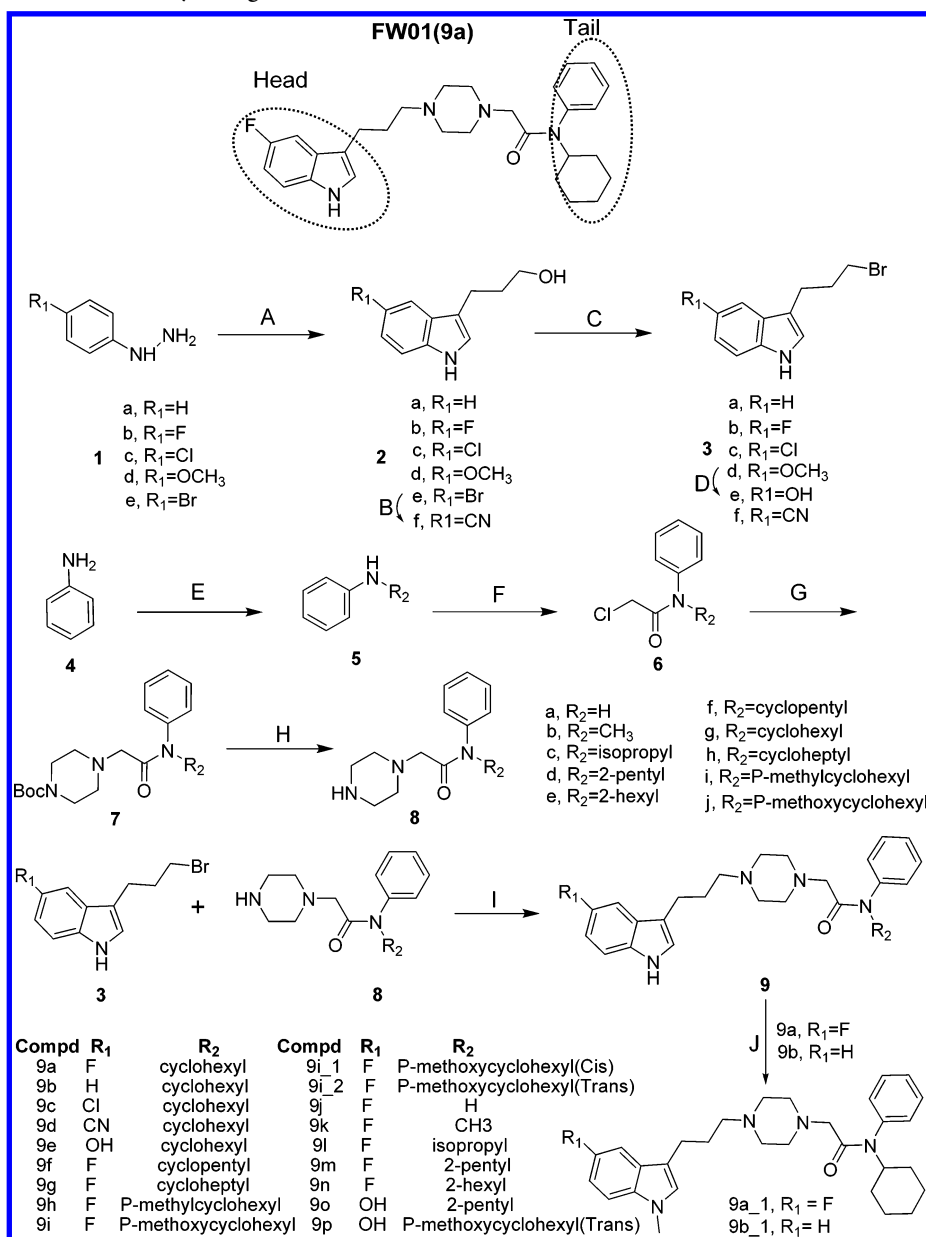
Serotonin (5-hydroxytryptamine, 5-HT), as a specific endogenous neurotransmitter, plays an important role in a plethora of human physiological and pathological processes in the central nervous system (CNS), such as mood, sleep, cognition, memory, and chronic pain alleviation.¹ 5-HT exerts its effects via 5-HT receptors, which can be classified into seven subfamilies, 5-HT₁ to 5-HT₇.^{2–7} Among them, 5-HT_{1A}R has drawn particular attention because of its important therapeutic potentials for anxiety,^{8–11} depression,^{3,12,13} cognition impairment,^{11,13} and other psychiatric syndromes.^{3,14} The 5-HT_{1A}R agonists have also been found as effective treatments for neurological disorders (e.g., Parkinson's disease)^{2,14,15} and for extrapyramidal side effects (EPS).^{10,16–18} Recent findings showed that the 5-HT_{1A}R agonists could be the potential treatments for ischemic stroke.^{4,9,19} Medicines like buspirone, gepirone, tandospirone, and vilazodone that act as 5-HT_{1A}R partial agonists have been used for years as anxiolytics or antidepressants.^{1,2,20} The reported new 5-HT_{1A}R ligands, F-15599, which showed potent antidepressant activity, and F13640 as a potential treatment of chronic pain, have entered clinical trials.^{21–23} Given the large needs of 5-HT_{1A}R agonists as potential treatments for various health problems, it is important to design novel chemical

agents with higher binding affinities and better pharmacological profiles.

In our previous studies,^{24,25} we have put great efforts into designing novel 5-HT_{1A}R agonists through the combination of computational approaches (e.g., dynamic pharmacophore-based virtual screening) and experimental tests (e.g., [³⁵S]GTPγS binding assay). We obtained a series of lead compounds as 5-HT_{1A}R agonists, which have novel scaffolds and high binding affinities. The previous best compound, **FW01** (denoted as **9a** in Scheme 1) showed a high affinity for 5-HT_{1A}R-binding (i.e., K_i value of 51.9 nM and EC_{50} value of 160.80 nM). Our previous results²⁴ of docking compound **9a** into the agonist-binding site of 5-HT_{1A}R revealed that **9a** adopted an extended conformation and was hydrogen bonded with residue D3.32 (Figure S1, Supporting Information). The headgroup (i.e., indole ring) of **9a** was located at subpocket 1 (denoted as SP1 in Figure S1, and here after) around residues S5.42, F6.51, and F6.52 of 5-HT_{1A}R and the tail group packed with residues Y2.64, F3.28, and W7.40 at subpocket 2 (denoted as SP2 in Figure S1, and here after) of 5-HT_{1A}R. Such a mode of 5-HT_{1A}R-**9a** binding is generally

Received: March 27, 2015

Published: July 1, 2015

Scheme 1. Synthetic Route for Newly Designed 9a Derivatives^a

^aReagents and conditions: (A) dihydropyran, DMAC/4% H_2SO_4 , reflux; (B) CuCN, DMF, 130 °C, reflux; (C) CBr_4 , PPh₃, DCM; (D) BBr₃, DCM, −78 °C; (E) Ketones, Zn, AcOH/ H_2O , reflux; (F) Chloroacetyl chloride, TEA, DCM; (G) Boc-piperazine, K_2CO_3 , CH_3CN , reflux; (H) TFA, DCM (I) K_2CO_3 , CH_3CN , reflux, 85 °C; (J) NaH, CH_3I , DMF, 65 °C, reflux.

consistent with the observed binding modes of other GPCR–ligand complexes and receptor–activation as reported in the X-ray crystal structures.^{2,26–28} Structurally, the headgroup of **9a** is connected to the central piperazine group through rotatable bonds and the similar intramolecular connection for the tail group of **9a** (Scheme 1). At the SP1 of 5-HT_{1A}R, the headgroup of **9a** could be hydrogen bonded with the side chain of residue S5.42 through either its –NH or –F atom. On the basis of these observed features, we wonder that how flexible the headgroup of **9a** could be when packing with the surrounding residues of 5-HT_{1A}R. Similarly, we also wonder whether or not the packing between the tail group of **9a** and SP2 of 5-HT_{1A}R can be tuned to the best possibility. Tuning of these local intermolecular interactions, if further explored, can very possibly provide new clues of structural modifications

of **9a**, which will definitely help us design higher-affinity agonists of 5-HT_{1A}R.

In the present study, we tested the binding flexibility of compound **9a** at the agonist-binding site of 5-HT_{1A}R by large-scale molecular dynamics (MD) simulations and conformational analysis on the 5-HT_{1A}R–**9a** binding structure. On the basis of the newly observed flip-packing phenomena between structural parts (i.e., headgroup and tail group) of **9a** and the subpockets (SP1 and SP2) of 5-HT_{1A}R, we designed a set of new derivatives of **9a** by substituting its headgroup and tail group, and by predicting their binding free energies with 5-HT_{1A}R. These newly designed **9a** derivatives were then synthesized, and tested for binding and functional assays. Through the tuning of 5-HT_{1A}R–ligand binding flexibility and our wet-experimental studies, we discovered a new series of higher-affinity agonists of 5-HT_{1A}R,

with ~50-fold increase in binding affinity (lowest K_i value of 1.01 ± 0.1 nM) and ~25-fold improvement of receptor-agonizing function (smallest EC_{50} value is 6.53 nM).

MATERIALS AND METHODS

Molecular Dynamics Simulations. In order to test how flexible compound **9a** is at the agonist-binding site of 5-HT_{1A}R, we performed MD simulations on the 5-HT_{1A}R-**9a** binding structure at the environment of the POPC lipid bilayer and the surrounding water molecules, which mimics the physiological condition of the receptor. The binding structure of the 5-HT_{1A}R-**9a** complex was derived directly from our previous studies on the modeling of 5-HT_{1A}R and its binding with **FW01**, and the simulation system was set up in a similar way as that described in our previous study.²⁹ In brief, the 5-HT_{1A}R-**9a** complex was inserted into a POPC lipid bilayer by using the inflated GRO method.³⁰ Meanwhile, the area per lipid was maintained to ~75 Å. Then, the system was solvated into a SPC water box.³¹ Na⁺ and Cl⁻ ions were randomly placed to neutralize and maintain the system ionic concentration of 154 mmol/L. In total, the system contains 37,610 atoms, including **9a**, 5-HT_{1A}R, 121 POPC lipids, 9,442 SPC water molecules, and 26 Na⁺ and 38 Cl⁻ ions. The MD simulations were performed using GROMACS 4.5.1 package.³² GROMOS96 53A6 force field in combination with the Berger lipid parameter for the POPC molecules³³ was used for the whole simulation. For the force field parameters of **9a**, the topology was prepared with PRODRG,²⁸ and the CHelpG partial charge was calculated using Gaussian 09³⁴ with the DFT/B3LYP/6-311g** basis set.

After the initial system was set up, 1,000 steps of steepest decent and 200 steps of conjugate gradient energy minimization were performed to remove the energetically unfavorable contacts. After that, the whole system was gradually heated from 0 to 310 K using velocity rescaling and equilibrated for 1.0 ns in the NPT ensemble with the protein and ligand restrained. The Nose-Hoover^{35,36} and Parrinello-Rahman methods^{37,38} were applied to maintain the system's temperature at 310 K and pressure of 1 bar, respectively. Then, the equilibration was continued for another 500 ps without any restrains. After that, the system was used for further unrestrained 200 ns MD simulations. During the simulation NPT ensemble, periodic boundary conditions were applied. The LINCS algorithm was adopted to constrain all bonds.³⁹ The partial-mesh Ewald (PME) algorithm⁴⁰ with a grid size of about 1 Å was applied to deal with the long-range electrostatic interactions. The van der Waals interactions were treated by using a cutoff of 12 Å. All the simulations were performed with a time step of 2 fs, and the coordinates were saved every 2 ps for later analysis. A similar strategy has been successfully applied in the studies of other biomacromolecule systems.^{41–44}

On the basis of the trajectory of MD simulations on the 5-HT_{1A}R-**9a** binding structure, we tracked the hydrogen bonding distance between the side chain of S5.42 (oxygen atom at -OH group) and the nitrogen atom of -NH group or -F atom of **9a**.

Docking 9a Derivatives into 5-HT_{1A}R Agonist-Binding Site. In order to see how compatible the substitutes of the headgroup and the tail group of compound **9a** are with both subpockets (SP1 and SP2), we performed molecular docking operations to dock all the **9a** derivatives into the agonist-binding site of 5-HT_{1A}R. Autodock4.2⁴⁵ and AutoDockTools version 1.5.6⁴⁶ (ADT) were applied for molecular docking. The docking files were prepared for both ligands and the receptors through the

tool ADT. For the ligands, the Gasteiger charges were assigned, and the nonpolar hydrogen atoms were merged into the attached carbon atoms. The rigid root of each ligand was defined automatically. The backbones and the amide bonds were allowed to rotate. The total number of the rotatable bonds of our ligands was counted to be about 14. For the receptors, the Gasteiger charges were added and the nonpolar hydrogen atoms were merged. Two typical conformations from the conformational analysis were selected as the target receptor (see Supporting Information for the coordinates of these conformations). The grid box was centered in the orthosteric agonist-binding site of 5-HT_{1A}R. The box size was set large enough to cover all the residues involved in agonist binding. The spacing between grid points was 0.375 Å.

The LGA (Lamarckian Genetic Algorithm) search algorithm was adopted to search for the best conformers. During the docking processes, the total energy evaluations were increased to 25,000,000, which is 10-fold of the default value to achieve a more thorough conformation search for all **9a** derivatives with an unusually large number of rotatable bonds. Gene mutation and the crossing over rate were set to 0.02 and 0.80, respectively. For each cycle, the top two individuals were allowed to survive to the next generation. A total of 100 instead of 10 (default value) LGA runs were launched for every compound. All the generated 100 conformers were ranked according to the calculated binding free energies (ΔG_{bind}) and also classified using the cluster analysis function of ADT with a threshold of root-mean-square deviation (RMSD) value of 2.0 Å. Those conformations with both the distance between the oxygen atom of the side chain of S5.42 and the nitrogen atom of -NH group or -F atom of **9a** derivatives and the distance between the oxygen atom of the side chain of D3.32 and the proton atom of the piperazine group of **9a** derivatives less than 3.5 Å were selected as initial candidates and were counted for the percentage over the total number of selected candidates.

First-Principles Calculations. As mentioned above, the headgroup of **9a** has two options (-NH or -F) to hydrogen bonding with the -OH group at the S5.42 side chain of 5-HT_{1A}R. In order to evaluate the contribution of this hydrogen bonding from different substituents at the headgroup of **9a** derivatives, we performed first-principles calculations by the quantum mechanics (QM) method implemented inside the Gaussian 09 package.⁴⁷ For this purpose, we used an F-substituted indole molecule to represent the headgroup of **9a** and a methanol molecule to mimic the S5.42 side chain of 5-HT_{1A}R. Such simplification can still reasonably represent the actual situation of this hydrogen bonding interaction and are within the acceptable molecular size for usual QM calculations. The first-principles calculations were also performed for different head groups of **9a** derivatives. The possible hydrogen binding options for each headgroup of each **9a** derivative and the methanol molecule were explored by these procedures. First, the hydrogen bonding options were searched using the mixed torsional/low-mode sampling method provided by Schrodinger Suite 2013⁴⁸ with OPLS2005 force field. A total of 100,000 options for each pair of molecules were visited during the stochastic search. Then, the conformers were fully optimized using the DFT method with Jaguar in the same Suite 2013. The B3LYP hybrid exchange-correlation functional and the 6-31+G* basis set were adopted for the optimization. For each option of hydrogen bonding, the dihedral angle between the plane of the headgroup and the C_α-hydroxyl plane of the methanol was further scanned with an interval of 15° at the same QM level as described before.

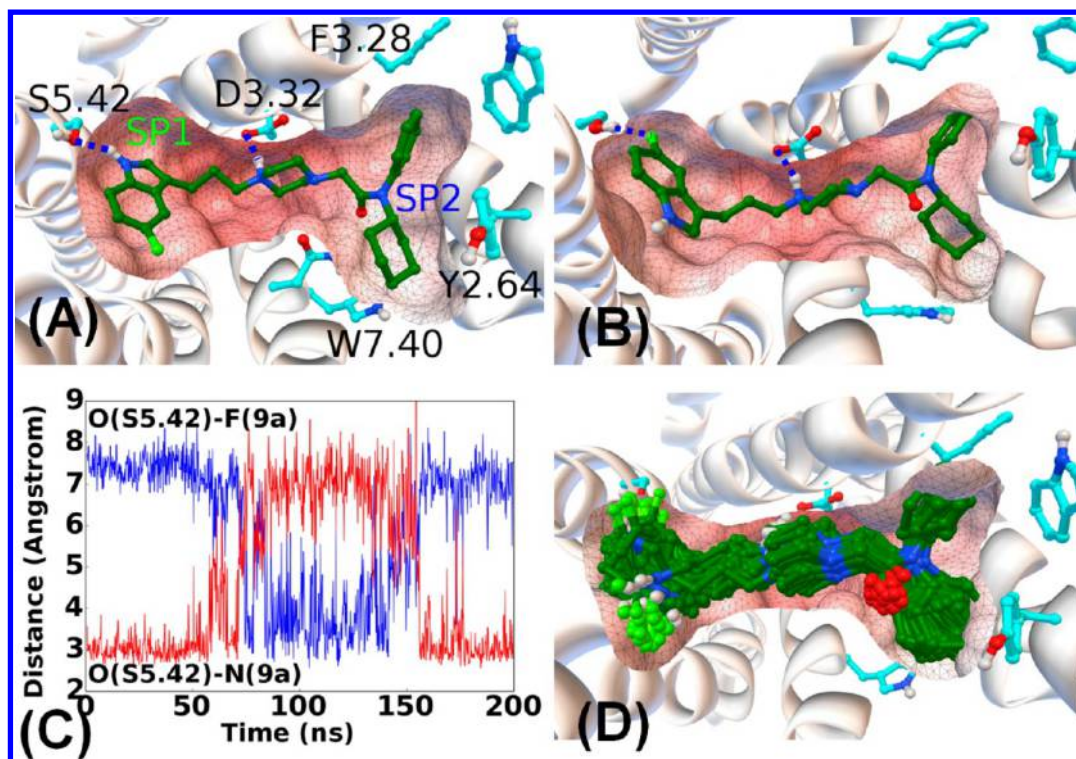


Figure 1. Flip-packing phenomenon for the headgroup of **9a** observed from the trajectory of 200 ns MD simulations on 5-HT_{1A}R–**9a** binding structure. (A) **9a** at the agonist-binding site of 5-HT_{1A}R before the flip of its headgroup, in which the –NH group is hydrogen bonded with the –OH group at the S5.42 side chain of 5-HT_{1A}R (i.e., HB_{S5.42–1}, –O···H–N–). 5-HT_{1A}R is represented as white ribbon, and key residues within 5 Å of **9a** are shown in ball-and-stick (cyan), while **9a** is shown in ball-and-stick (green). (B) **9a** at the binding site of 5-HT_{1A}R after the flip of its headgroup, in which the –F atom is hydrogen bonded with the –OH group at the S5.42 side chain of 5-HT_{1A}R (i.e., HB_{S5.42–5'}, –O–H···F). (C) O(S5.42)–N(**9a**) represents the tracked distance between the oxygen atom at the S5.42 side chain and the nitrogen atom at the headgroup of **9a** (red line) and O(S5.42)–F(**9a**) for the tracked distance between the oxygen atom at the S5.42 side chain and the fluorine atom at the headgroup of **9a** (blue line) during the 200 ns MD simulations with the interval of 200 ps. (D) Superimposed conformations of **9a** at the binding site of 5-HT_{1A}R, which were derived from the trajectory of first 150 ns MD simulations with an interval of 2 ns.

The obtained conformations were then optimized by using the Gaussian09 package⁴⁹ with the DFT method of B3LYP/6-311+G** in gas phase. The single point energy and the formation enthalpy for each pair of hydrogen bonding were calculated using a larger basis set (i.e., aug-cc-pVTZ set) with polarizable continuum model (PCM) in aqueous solution. After this calculation, the population analyses of the molecular orbitals were carried out, and the charges for each pair of hydrogen bonding were fitted to the electrostatic potential using the CHelpG scheme.

Chemical Synthesis. Each of the virtually designed **9a** derivatives was synthesized according to the route as shown in Scheme 1. The indolepropanol moiety **2** was prepared from the corresponding phenylhydrazine derivative via Fischer indole synthesis. The generated alcohol intermediate was then converted to bromo derivative **3** with carbon tetrabromide and triphenylphosphine.⁵⁰ The 5-cyanoindole propanol, **2f**, was prepared from 5-bromo compound **2e** by the treatment with copper(I) cyanide in DMF. Compound **3e** was obtained from **3d** via the demethylation reaction. Starting from the aniline, **4**, the intermediate **8** was synthesized. First, compound **4** was treated with a ketone derivative in the reductive amination condition to achieve a good yield of the secondary *N*-alkylarylamine, **5**. Subsequently, the amine was acylated with acyl chloride to obtain compounds **6**, followed by alkylation with *N*-Boc-piperazine to yield derivative **7**, and then, the deprotection of the *N*-Boc-piperazine moiety of compound **7** lead to the formation of

intermediate **8**. With the combination of alkylindole moiety **3** and *N*-substituted piperazine **8**, each of the **9a** derivatives was synthesized in the presence of potassium carbonate and acetonitrile. In addition, compounds **9a_1** and **9b_1** were obtained via methylation of **9a** and **9b**, respectively. Structures of all the **9a** derivatives were verified by ¹H and ¹³C NMR spectra. The detailed spectral data are provided in the Experimental Section of the Supporting Information.

Binding Assays. All the synthesized **9a** derivatives were subjected to competitive binding assays for the human dopamine (D₁, D₂, and D₃) and serotonin (5-HT_{1A}, 5-HT_{2A}) receptors in order to validate our virtual design based on the MD simulations and the first-principles calculations and also to wet-experimentally test how selective these synthesized **9a** derivatives are for 5-HT_{1A}R over 5-HT_{2A}R and dopamine receptors. The binding assays were performed by using membrane preparation obtained from stable transfected HEK293 cells as described in our previous studies.^{39,51} For each **9a** derivative, the initial screening was conducted with a 10 μM compound to test its inhibition on the binding of a tritiated radioligand to each of these receptors. A compound that inhibited binding by more than 85% was further assayed for IC₅₀. The K_i value was calculated based on this relation: $K_i = IC_{50} / (1 + C/K_d)$. [³H]-SCH23390, [³H]-Spiperone, [³H]-8-OH-DPAT, and [³H]-Ketanserin were used as standard radioligands for D₁, D₂/D₃, 5-HT_{1A}, and 5-HT_{2A} receptors, respectively. The binding reaction was conducted in duplicated tubes in a 200 μL of binding

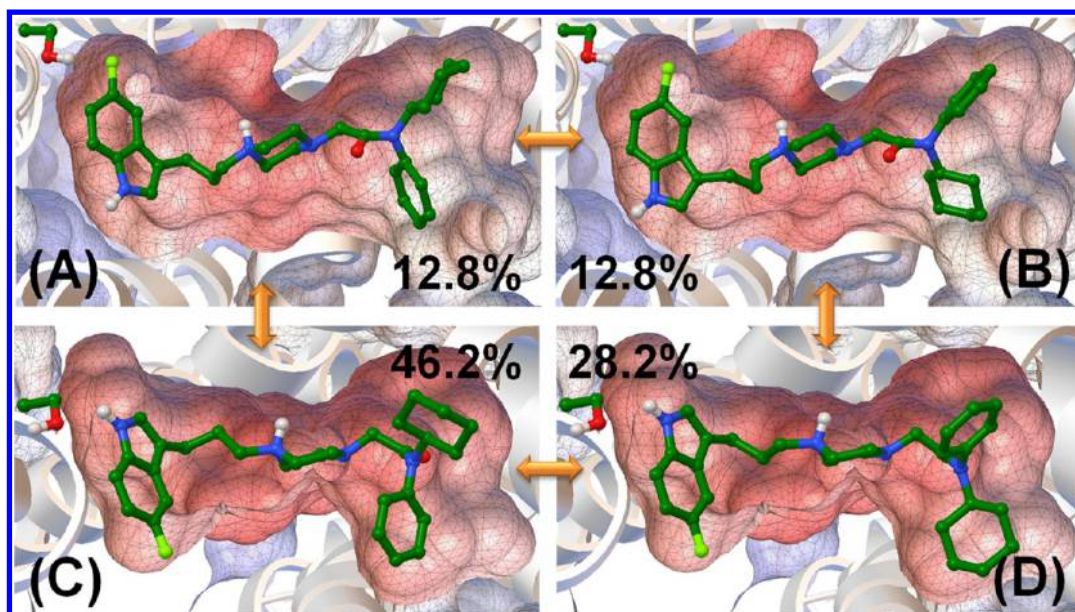


Figure 2. Typical four different orientations for **9a** at the agonist-binding site of 5-HT_{1A}R. The binding site is represented as a meshed molecular surface, and the receptor is represented as a ribbon. The **9a** molecule is shown in ball-and-stick. (A) Headgroup of **9a** is hydrogen bonded through its $-F$ atom with the $-OH$ group at the S5.42 side chain ($HB_{S5.42-5}$ $-O-H\cdots F$), while the tail group of **9a** takes the phenyl-down pose. (B) Headgroup of **9a** is orientated the same as that in (A) (i.e., $HB_{S5.42-5}$ $-O-H\cdots F$), while its tail group takes the phenyl-up pose. (C) Headgroup of **9a** is hydrogen bonded through its $-NH$ atoms with the $-OH$ group at the S5.42 side chain ($HB_{S5.42-1}$ $-O\cdots H-N-$), and the tail group of **9a** takes the phenyl-down pose. (D) Headgroup of **9a** has the same option of hydrogen bonding (i.e., $HB_{S5.42-1}$ $-O\cdots H-N-$) as that in (C), but the tail group of **9a** takes the phenyl-up pose. The population weighted binding free energies (ΔG_{bind}) from molecular docking are -10.55 kcal/mol for (A), -10.45 kcal/mol for (B), -11.00 kcal/mol for (C), and -10.87 kcal/mol for (D).

buffer containing 50 mM Tris and 4 mM of $MgCl_2$ (pH 7.4) at 30 °C for 50 min with increasing concentrations (within the range of 1 nM \sim 100 μ M) of the testing compound in the presence of 0.7 nM [3H]SCH23390, [3H]Spiperone, [3H]8-OH-DPAT, or [3H]Ketanserin. The reaction was started by addition of membranes (15 μ g/tube), stopped by rapid filtration through a Whatman GF/B glass fiber filter, and subsequently washed with cold buffer. Nonspecific binding was determined by parallel incubations with 10 μ M SCH23390 for D₁R, 10 μ M Spiperone for D₂R/D₃R, 10 μ M 5-HT for 5-HT_{1A}R, and 10 μ M butaclamol for 5-HT_{2A}R. Scintillation cocktail was added, and the radioactivity was determined in a MicroBeta liquid scintillation counter. The IC_{50} and K_i values were calculated by nonlinear regression using a sigmoidal function.

[^{35}S]GTP γ S Binding Assays. To test that our synthesized **9a** derivatives are able to activate the 5-HT_{1A}R, which in turn binds the intracellular G protein for signal transduction over the membrane, we performed a standard [^{35}S]GTP γ S binding assay for each of the **9a** derivatives. The [^{35}S]GTP γ S binding assay was performed as described in our previous studies.^{29,39,52} Briefly, the [^{35}S]GTP γ S binding reaction was conducted at 30 °C for 30 min with 30 μ g of membrane protein in a final volume of 200 μ L with various concentrations of each of the tested compound. The natural substrate of 5-HT_{1A}R, serotonin, was used as a positive control. The binding buffer contains 50 mM Tris (pH 7.4), 5 mM $MgCl_2$, 1 mM ethylenediaminetetraacetic acid (EDTA), 100 mM NaCl, 1 mM DL-dithiothreitol (DTT), and 40 μ M guanosine triphosphate (GDP). The [^{35}S]GTP γ S binding reaction was initiated by adding [^{35}S]GTP γ S (final concentration of 0.1 nM). Nonspecific binding was measured in the presence of 100 μ M 5'-guanylimidodiphosphate (Gpp(NH)p). The [^{35}S]GTP γ S binding reaction was terminated by the addition of 1 mL of ice-cold washing buffer, was rapidly filtered with GF/C glass fiber

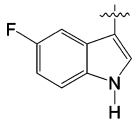
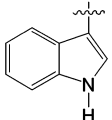
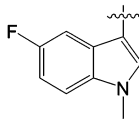
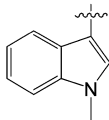
filters (Whatman), and then washed three times. Radioactivity was determined by liquid scintillation counting.

RESULTS AND DISCUSSION

Flip-Packing of **9a** Head Group at SP1 Subsite in 5-HT_{1A}R.

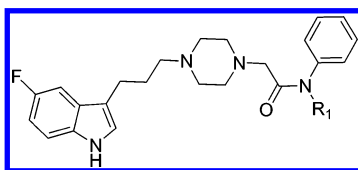
Depicted in Figure 1 is the dynamic orientation of lead compound **9a** at the agonist binding site of 5-HT_{1A}R, which was tracked through the 200 ns MD simulations. Figure 1A and B shows the two typical options of hydrogen bonding between the headgroup of **9a** and the $-OH$ group of the S5.42 side chain at the subpocket SP1 of 5-HT_{1A}R: $-NH$ at the headgroup of **9a** is hydrogen bonded with $-OH$ group at S5.42 side chain through the option of $-O\cdots H-N-$ (denoted as $HB_{S5.42-1}$ and here after), and the $-F$ atom at the headgroup of **9a** is hydrogen bonded with the $-OH$ group at S5.42 side chain (Figure 1B) in the option of $-O-H\cdots F$ (denoted as $HB_{S5.42-5}$ and here after). In order to see whether these two options of hydrogen bonding are dynamically exchangeable, we tracked the distances during the MD simulations for these two hydrogen-bonding interactions. As shown in Figure 1C (red curve), the $HB_{S5.42-1}$ option of hydrogen bonding lasted for the first \sim 50 ns of MD simulations, as the tracked O(S5.42)–N(**9a**) distance fluctuated flatly around 3 Å. Such a hydrogen bonding interaction was flipped gradually and was replaced by the $HB_{S5.42-5}$ option of hydrogen bonding (Figure 1C, blue curve), which lasted until \sim 150 ns along the MD trajectory. The second flip, i.e., from $HB_{S5.42-5}$ to $HB_{S5.42-1}$, happened at once and lasted until the end of MD simulations. Figure 1D depicts the superimposed conformations of **9a** at the binding site of 5-HT_{1A}R, which were derived from the first 150 ns of MD trajectory with the interval of 2 ns. These dynamic properties of the 5-HT_{1A}R–**9a** binding structure demonstrated that the headgroup of **9a** flipped between two options of hydrogen bonding interaction with the S5.42 residue, while located always inside SP1 of 5-HT_{1A}R.

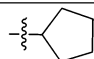
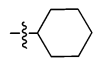
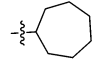
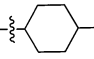
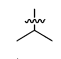
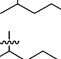
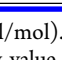
Table 1. Wet-Experimentally Measured 5-HT_{1A} Binding Affinities (K_i , nM, or percentage for the displacement of the radioligand at 10 μ M) for Designed 9a Derivatives Based on Observed Flip-Packing of Head Group (Scheme 1) of 9a from MD Simulations and Molecular Docking^a

Compound	9a	9b	9a_1	9b_1
HB options	2	1	1	0
Head group				
HB _{S5.42-1} / HB _{S5.42-5} *	2.9:1	7.3:1	1:1.7	1:1.1
ΔG_{bind} **	-10.83	-10.29	-10.09	-9.02
K _i	51±16	314±7	542±3	82.29%

^aAlso listed are the calculated binding free energies (ΔG_{bind} , kcal/mol). *Ratio of hydrogen bonding HB_{S5.42-1}/HB_{S5.42-5} counted from results of molecular docking operations. **Each calculated free energy value was the weighted average based on its population.

Table 2. Wet-Experimentally Measured 5-HT_{1A} Binding Affinities (K_i , nM) for Designed 9a Derivatives Based on the Observed Flip-Packing of the Tail Group (Scheme 1) of 9a from MD Simulations and Molecular Docking^a



Compound	Carbon atoms in R ₁	R ₁ group	Phenyl_down/ Phenyl_up*	ΔG_{bind} **	K _i
9f	5		1.32:1	-10.33	42±5
9a	6		1.44:1	-10.83	51±16
9g	7		1.85:1	-10.55	192±11
9h	7		1:2.96	-10.25	88±13
9j	0	H	0.24:1	-9.64	103±3
9k	1	CH ₃	0.45:1	-9.89	51±10
9l	3		0.59:1	-10.23	41±4
9m	5		1.10:1	-10.31	3.5±0.1
9n	6		1.00:1	-10.18	41±5

^aAlso listed are the calculated binding free energies (ΔG_{bind} , kcal/mol). *Ratio of phenyl position phenyl-down/phenyl-up counted from the results of molecular docking operations. **Each calculated free energy value was the weighted average based on its population.

Using the OPLS2005 force field implemented in Schrodinger Suite 2013,¹⁸ the minimum energy path (MEP) for the rotation of the headgroup of 9a was searched without the presence of 5-HT_{1A}R, and we found that the energy barrier for the flip of the 9a headgroup is only ~1.0 kcal/mol (Figure S2, Supporting Information). This indicates that the headgroup of 9a is readily able to rotate, supporting the observed flip-packing events along the MD simulations on the 5-HT_{1A}R–9a binding structure (Figure 1).

Four Possible Orientations of 9a for 5-HT_{1A}R–9a Binding. Since the headgroup of 9a can flip inside the SP1 of

the receptor (Figure 1A and Figure S1, Supporting Information), we wanted to know how many possible typical orientations of 9a there are at the agonist-binding site of 5-HT_{1A}R and their contributions to the overall 5-HT_{1A}R–9a binding. According to our results of molecular docking, there are four possible orientations of 9a at the agonist-binding site, which contribute significantly to the overall receptor binding (Figure 2). Besides the observed two options of hydrogen bonding with the S5.42 residue by the headgroup of 9a, we also found that the tail group (Scheme 1) of 9a can also pack in two typical options with the

surround residues at SP2 of 5-HT_{1A}R, i.e., the phenyl group of **9a** packs mainly around F3.28 residue (as labeled in Figure 1A), denoted as phenyl-up pose, or the phenyl group of **9a** mainly packs around W7.40 (as labeled in Figure 1A) of 5-HT_{1A}R, denoted as phenyl-down pose. Through cluster analysis on the selected conformational candidates of **9a** from molecular docking, we found that the HB_{S5.42-1} option of hydrogen bonding occupied 74.4% of all the conformations of **9a** at the binding site of 5-HT_{1A}R, while 25.6% for the HB_{S5.42-5} option. The phenyl-down pose for the tail group of **9a** takes 59.0% among all the binding conformations of **9a** at the SP2 of the binding site of 5-HT_{1A}R and 41.0% for the phenyl-up option of the **9a** tail group. As observed, the orientation of **9a** with HB_{S5.42-5} and the phenyl-down pose at the binding site (Figure 2A) takes only 12.8% for the population of **9a** binding conformations and has the calculated binding free energy (ΔG_{bind}) of -10.55 kcal/mol. The orientation of **9a** with HB_{S5.42-5} and the phenyl-up pose has also 12.8% of the whole population and has the ΔG_{bind} value of -10.45 kcal/mol (Figure 2B). The **9a** orientation with HB_{S5.42-1} and phenyl-down pose (Figure 2C) at the binding site of 5-HT_{1A}R takes 46.2% with the ΔG_{bind} value of -11.0 kcal/mol, and the ΔG_{bind} value of -10.87 kcal/mol for the HB_{S5.42-1} plus phenyl-up pose (Figure 2D). The total binding free energy contributed from these four possible orientations of **9a** at the agonist-binding site of 5-HT_{1A}R is -10.83 kcal/mol.

Testing the Observed Flip-Packing of **9a** Head Group.

In order to test that the observed flip-packing of the **9a** head-group at the SP1 site of 5-HT_{1A}R and the importance of the hydrogen bonding between the **9a** headgroup and the S5.42 residue to the affinity of 5-HT_{1A}R–**9a** binding, we virtually designed three **9a** analogs. These are **9b** with the HB_{S5.42-5} blocked (i.e., removed –F atom) (Scheme 1, Table 1), **9a_1** with HB_{S5.42-1} blocked (i.e., added methyl substituent to the nitrogen atom at the head-group), and **9b_1** (no hydrogen bonding with S5.42 residue). Using the same protocols of molecular docking as described above, we found that **9b** takes the HB_{S5.42-1} option up to 87.9%, that is, the 7.3:1 ratio for the HB_{S5.42-1} over the non-HB_{S5.42-1}, and the calculated value of ΔG_{bind} for **9b** is -10.29 kcal/mol. The calculated ΔG_{bind} values for **9a_1** (ratio of HB_{S5.42-5} over non-HB_{S5.42-5} as 1.7:1) and **9b_1** (headgroup flips equally toward S5.42 residue of 5-HT_{1A}R) are -10.09 and -9.02 kcal/mol, respectively. On the basis of these calculated values of ΔG_{bind} , we predicted that the order of receptor-binding affinity for these four compounds should be **9a** > **9b** > **9a_1** > **9b_1**. We then submitted these four compounds to chemical synthesis (as shown in Scheme 1) and binding assays (as described above). The wet-experimental measurements are listed in Table 1. Interestingly, the measured binding affinities of these four compounds followed same decreasing order as **9a** > **9b** > **9a_1** > **9b_1**, i.e., increasing K_i (nM) value or percentage for the displacement of radioligand at $10 \mu\text{M}$. The consistency between our computational predictions and wet-experimental results strongly suggests that the hydrogen bonding between **9a** and the S5.42 residue of 5-HT_{1A}R is very important for agonist-binding, and the HB_{S5.42-1} option of hydrogen bonding contributes more to the agonist affinity than that from the HB_{S5.42-5} option.

Testing the Flexibility of **9a Tail Group at SP2 Site.** As found in the above **9a** analogs (**9b**, **9a_1**, **9b_1**), the tail group of **9a** can take the pose as both phenyl-up and phenyl-down at the SP2 subsite of 5-HT_{1A}R (Figure 2), and we wanted to test how flexible the tail group is. The similar MEP for the rotation of the tail group of **9a** was also searched without the presence of 5-HT_{1A}R, and we found that the energy barrier for the rotation of

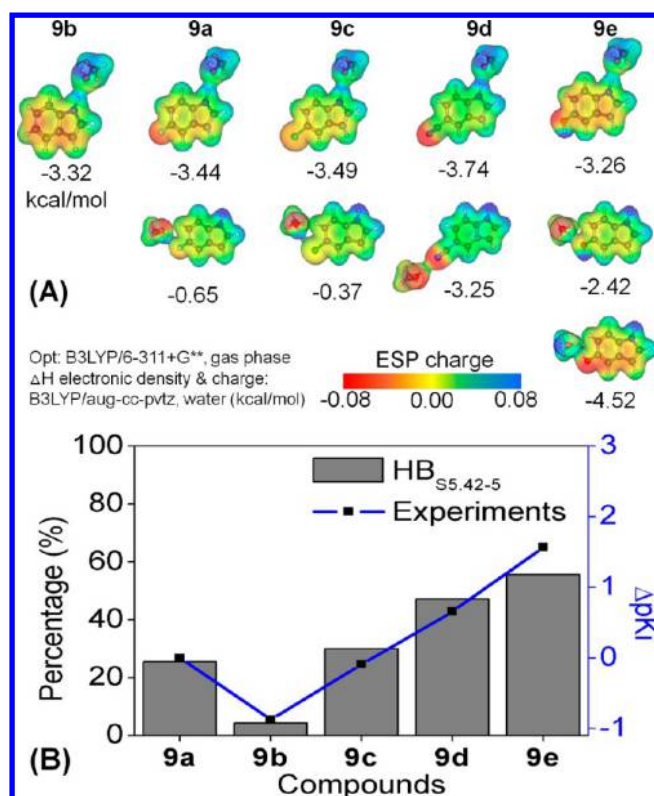
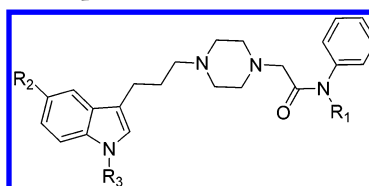


Figure 3. Hydrogen bonding energies from first-principles calculations on different head groups of **9a** derivatives (**9a**, **9b**, **9c**, **9d**, and **9e**) hydrogen bonded with the –OH group of the S5.42 side chain (which is mimicked as methanol). (A) First row shows the electrostatic potential (ESP charge) on the molecular surface for each headgroup of each **9a** derivative for the hydrogen bonding HB_{S5.42-1}. Second and third rows show the ESP charge for the hydrogen bonding HB_{S5.42-5}. The calculated energy (kcal/mol) for each pair of hydrogen bonding interaction is also shown. (B) Bar plot shows the ratio of hydrogen bonding HB_{S5.42-5} counted from the results of molecular docking for **9a** derivatives. Blue line shows the difference (ΔpK_i) between each **9a** derivative and that of **9a** for pK_i (i.e., $-\log K_i$) as measured for the binding with human 5-HT_{1A} receptor.

the **9a** tail group is as small as ~ 1.3 kcal/mol (Figure S3, Supporting Information). We first changed the size of the hexacycle substituent at the tail group, i.e., the penta-cycle substituent for **9f**, heptacycle substituent for **9g**, and **9h**, by adding a methyl-substituent at the hexacycle group at the tail of **9a** (Scheme 1). Results of docking these three molecules (**9f**, **9g**, and **9h**) into the agonist-binding site of 5-HT_{1A}R showed that these three analogs can still have the options of phenyl-up and phenyl-down for the tail at SP2 site (Figure S4, Supporting Information). However, results of binding assays (Table 2) showed that these three analogs have decreased affinities with 5-HT_{1A}R, suggesting that the SP2 subsite in the receptor does not accept larger-size alkyl-cycle substituents. For this reason, we designed more **9a** derivatives by changing the hexacycle substituent with smaller alkyl-chain substituents, namely, **9j**, **9k**, **9l**, **9m**, and **9n** (Scheme 1). The results of binding assays on these **9a** derivatives showed that **9m**, with the pentyl substituent at the tail group, has better affinity for 5-HT_{1A}R-binding, i.e., $K_i = 3.5 \pm 0.1$ nM (Table 2), which corresponds to the ratio of phenyl-up/phenyl-down of the tail group of 1.10:1 from molecular docking operations.

Rational Design of Higher-Affinity **9b Derivatives.** Encouraged by the above preliminary testing results on the

Table 3. Wet-Experimentally Measured Binding Affinities (K_i , nM, or percentage for displacement of radioligand at 10 μ M) for All Newly Designed 9a Derivatives with Dopamine Receptors (D_1 , D_2 , and D_3) and Serotonin Receptors (5-HT_{1A} and 5-HT_{2A})



Compd	R ₁	R ₂	R ₃	$K_i \pm \text{SEM (nM)}^a$				
				D ₁	D ₂	D ₃	5-HT _{1A}	5-HT _{2A}
FW01 (9a)		F	H	34.1%	31.7%	2161±2	51±16	206.7±7
9b		H	H	26.6%	34.7%	73.2%	314±7	200±16
9a_1		F	CH ₃	ND	ND	ND	542±3	520.1±11
9b_1		H	CH ₃	ND	ND	ND	82.29%	76.68%
9c		Cl	H	60.35%	75.76%	666±33	51±7	1936±15
9d		CN	H	9.5%	43.2%	77.7%	9.2±1	1365±42
9e		OH	H	5.13%	37.85%	83.99%	1.1±0.1	163±9
9f		F	H	42.3%	19.8%	795±1.3	42±5	155±5
9g		F	H	25.3%	25.2%	1107±40	192±11	373±22
9h		F	H	34.0%	24.4%	409 ±53	88±13	163±13
9i		F	H	27.28%	76.44%	83.84%	11±2	363±94
9i_1		F	H	13.1%	22.0%	72.6%	127±2	122±22
9i_2		F	H	6.0%	54.5%	1375±3	1.6±1	89.6±12
9j	H	F	H	18.08%	9.13%	52.99%	103±3	75.30%
9k	CH ₃	F	H	1.63%	9.49%	57.21%	51±10	169±5
9l		F	H	1.48%	21.8%	73.3%	41±4	230±23
9m		F	H	43.7%	46.9%	255 ±34	3.5±0.1	60±15
9n		F	H	40.53%	74.94%	874±7	41±5	971±11
9o		OH	H	5.13%	37.85%	83.99%	1.01±0.1	158±9
9p		OH	H	10.08%	1.61%	70.04%	1.05±0.3	350±16

^aBinding data are the mean values of five to six individual experiments with 5-HT_{1A} receptors each done in triplicate.

binding flexibility of 9a analogs at the agonist-binding site of 5-HT_{1A}R, we extended our efforts to design higher affinity agonists by tuning the observed flip-packing of the 9a headgroup

and the phenyl-up/phenyl-down poses of the 9a tail group. For this purpose, we designed three more 9a derivatives, namely, 9c with −Cl substituent at the original F atom position, 9d with

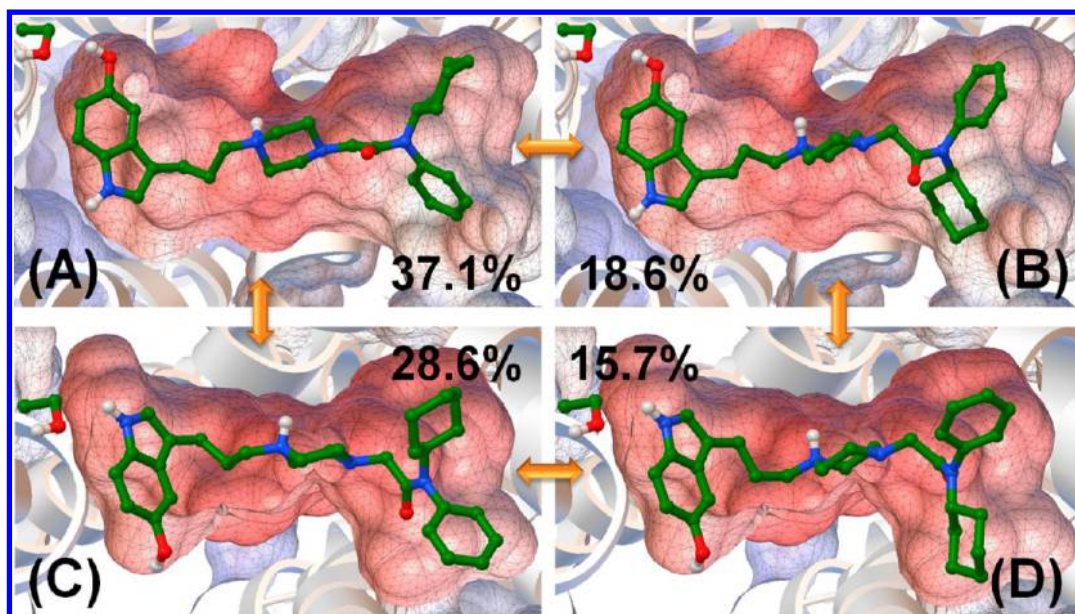


Figure 4. Most possible four orientations for **9e** at the agonist-binding site of 5-HT_{1A}R are shown in a similar style as that in Figure 2. (A) Headgroup of **9e** is hydrogen bonded through its $-\text{OH}$ atom with the $-\text{OH}$ group at the S5.42 side chain ($\text{HB}_{\text{S5.42-5}}-\text{O}\cdots\text{H}-\text{O}-$), while the tail group of **9a** takes the phenyl-down pose. (B) Headgroup of **9e** is orientated the same as that in (A) (i.e., $\text{HB}_{\text{S5.42-5}}-\text{O}\cdots\text{H}-\text{O}-$), while its tail group takes the phenyl-up pose. (C) Headgroup of **9e** is hydrogen bonded through its $-\text{NH}$ atoms with the $-\text{OH}$ group at the S5.42 side chain ($\text{HB}_{\text{S5.42-1}}-\text{O}\cdots\text{H}-\text{N}-$), and the tail group of **9e** takes the phenyl-down pose. (D) Headgroup of **9e** has the same option of hydrogen bonding (i.e., $\text{HB}_{\text{S5.42-1}}-\text{O}\cdots\text{H}-\text{N}-$) as that in (C), but the tail group of **9e** takes the phenyl-up pose. The population weighted binding free energies (ΔG_{bind}) from molecular docking are -11.61 kcal/mol for (A), -10.86 kcal/mol for (B), -10.67 kcal/mol for (C),; and -10.59 kcal/mol for (D).

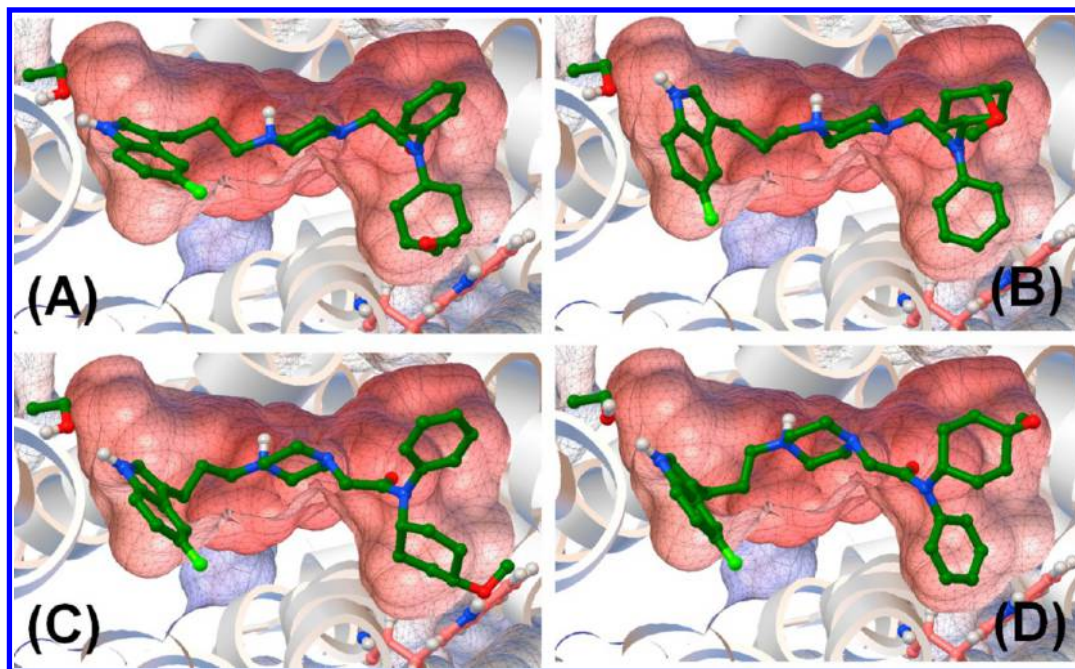


Figure 5. Most possible orientations for **9i_1** and **9i_2** at the agonist-binding site of 5-HT_{1A}R are shown in a similar style as that in Figure 2. (A) Headgroup of **9i_1** is hydrogen bonded through its $-\text{NH}$ atoms with the $-\text{OH}$ group at the S5.42 side chain ($\text{HB}_{\text{S5.42-1}}-\text{O}\cdots\text{H}-\text{N}-$), while the tail group of **9i_1** takes the phenyl-up pose. (B) Headgroup of **9i_1** is orientated the same as that in (A) (i.e., $\text{HB}_{\text{S5.42-1}}-\text{O}\cdots\text{H}-\text{N}-$), while its tail group takes the phenyl-down pose. (C) Headgroup of **9i_2** is hydrogen bonded through its $-\text{NH}$ atoms with the $-\text{OH}$ group at the S5.42 side chain ($\text{HB}_{\text{S5.42-1}}-\text{O}\cdots\text{H}-\text{N}-$), and the tail group of **9i_2** takes the phenyl-down pose. (D) Headgroup of **9i_2** has the same option of hydrogen bonding (i.e., $\text{HB}_{\text{S5.42-1}}-\text{O}\cdots\text{H}-\text{N}-$) as that in (C), but the tail group of **9i_2** takes the phenyl-up pose. The population weighted binding free energies (ΔG_{bind}) calculated from molecular docking are -10.25 kcal/mol for **9i_1** and -10.71 kcal/mol for **9i_2**.

a $-\text{CN}$ substituent, and **9e** with $-\text{OH}$ substituent (Scheme 1), i.e., playing the $\text{HB}_{\text{S5.42-5}}$ pattern of hydrogen bonding at the headgroup of **9a**. We performed the first-principles calculations on these three more derivatives and **9a** and **9b**. The results of the

QM calculations as shown in Figure 3 indicate that all these **9a** derivatives have at least one option of hydrogen bonding, i.e., $\text{HB}_{\text{S5.42-1}}$ and/or $\text{HB}_{\text{S5.42-5}}$. As the substituent at the original $-\text{F}$ atom of the headgroup changed from $-\text{H}$ to $-\text{F}$ to $-\text{Cl}$ to $-\text{CN}$

and to $-OH$, the chance of forming $HB_{SS,42-5}$ became higher (Figure 3A), and therefore, the total contribution from hydrogen bonding to the affinity should increase. On the basis of the results of these QM calculations and the ratio of $HB_{SS,42-5}/HB_{SS,42-1}$ from docking operations, we would predict that these **9a** derivatives have the order of 5-HT_{1A}R-affinity as **9b** < **9a** ~ **9c** < **9d** < **9e**. The results of binding assays on these synthesized **9a** derivatives are shown in Figure 3B and are also listed in Table 3. The measured K_i values for these **9a** derivatives confirmed the predicted order of affinity from QM calculations and molecular docking operations. Specifically, compound **9e** showed much higher affinity of 5-HT_{1A}R-binding, i.e., the K_i value is as low as 1.1 ± 0.1 nM, about a 50-fold increase in receptor-binding affinity when compared with that of **9a**.

Figure 4 depicts the four possible orientations of compound **9e** at the agonist-binding site of 5-HT_{1A}R, which were obtained by the same protocols as that applied on lead compound **9a** (Figure 2). These results suggest that the way of our rational design is reasonable.

Further tuning on the **9a** tail group has led to the design of **9i**. By adding a $-O-CH_3$ substituent to the para-position of the hexacycle part at the tail of **9a**, we synthesized compound **9i** (as shown in Scheme 1) and submitted it to the binding affinity assay. It turned out that **9i** has a higher affinity with 5-HT_{1A}R-binding than that of **9a**. As listed in Table 3 for **9i**, its $K_i = 11.0 \pm 2$ nM. Structurally, **9i** is a racemic mixture, that is, it has the *cis*-conformer (**9i_1**) and the *trans*-conformer (**9i_2**). In a similar way, we docked both of these two compounds into the agonist-binding site of 5-HT_{1A}R and found that the oxygen atom of $-O-CH_3$ at the tail group of **9i_2** can form one additional hydrogen bond with a W7.40 side chain of 5-HT_{1A}R (as shown in Figure 5C). On the basis of these docking results, we would predict that **9i_2** should have a higher affinity with 5-HT_{1A}R than that of **9i** itself. After both **9i_1** and **9i_2** were synthesized (as shown in Scheme 1), we again submitted these two compounds **9i_1** and **9i_2** to receptor-binding assays. The results of wet-experimental tests are listed in Table 3, and compound **9i_2** showed $K_i = 1.6 \pm 1$ nM, a higher affinity for 5-HT_{1A}R-binding than that of **9i**.

All-in-One Tuning for Design of Higher-Affinity Agonists.

As described above, the rationally designed **9e** and **9i_2** became the nM-level agonists of 5-HT_{1A}R. This is because these two higher-affinity agonists were designed either through taking advantage of the observed flip-packing phenomenon of the headgroup of **9a** at the SP1 subsite of 5-HT_{1A}R or through tuning the flexibility of the tail of **9a** at the SP2 subsite of the receptor. If we combined these two merits together, we wanted to see whether or not the all-in-one tuning of the binding flexibility at the agonist-binding site of 5-HT_{1A}R could help us make new active compounds. Following the same protocols as described above, i.e., through a combination of molecular docking and wet-experimental tests, we discovered new compounds **9o** and **9p** (as shown in Scheme 1), which have both the best hydrogen-bonding options at the headgroup and the best flexibility of the tail group (phenyl-up/phenyl-down poses). As listed in Table 3, both **9o** and **9p** showed nM-level affinities toward the 5-HT_{1A}R-binding, i.e., K_i values are 1.01 ± 0.1 and 1.05 ± 0.3 nM, respectively.

In addition, we also checked the 5-HT_{1A}R-activation abilities of our newly designed **9a** derivatives by performing the standard [³⁵S]GTPγS binding assays. Table 4 lists the results of the wet-experimental tests for some of our newly designed **9a** derivatives. As shown in Table 4, the most active compounds **9e**, **9i_2**, and

Table 4. Results of [³⁵S]GTPγS Assays (EC_{50} , nM) for Newly Designed **9a** Derivatives

compound	5-HT _{1A} R agonistic activity	
	EC_{50} (nM)	$E_{max}\%$
9a	106.80	133.14 ± 4.03
9c	43.63	124.16 ± 33.47
9d	6.53	105.23 ± 22.07
9e	24.42	110.42 ± 7.85
9f	287.11	86.75 ± 3.47
9h	46.73	100.77 ± 25.06
9i_2	11.95	116.83 ± 2.96
9m	29.67	105.52 ± 3.39
9o	15.81	80.32 ± 1.07
5-HT	1.7016	100

9o have EC_{50} values of 24.42, 11.95, and 15.81 nM, respectively. The much-lowered EC_{50} values of these compounds confirm again that our rationale to design higher-affinity agonists of 5-HT_{1A}R is successful.

Meanwhile, we also performed wet-experimental measurements for the affinities of our newly designed **9a** derivatives with subtype 5-HT_{2A}R and also for the dopamine receptors (D_1 , D_2 , and D_3), in order to test their selectivity about 5-HT_{1A}R. As listed in Table 3, the 5-HT_{2A}R/5-HT_{1A}R selectivity for our newly designed **9a** derivatives became higher as their binding affinities with 5-HT_{1A}R became higher. For example, the 5-HT_{2A}R/5-HT_{1A}R selectivity for **9a** is ~4-fold, and it goes up to ~33-fold for **9i**, to ~56-fold for **9i_2**, to ~148-fold for **9e**, and even to ~333-fold for **9p**. Additionally, all of our newly designed **9a** derivatives are also highly selective over dopamine receptors (Table 3). These data of selectivity suggest that the observed binding flexibility for **9a** derivatives at the subsites SP1 and SP2 of 5-HT_{1A}R is unique, and our tuning approaches can be generally applied in the design of high-affinity agonists targeting other subtype 5-HT receptors.

CONCLUSION

In summary, we observed a dynamic flip-packing phenomenon for the headgroup of lead compound **9a** through large-scale molecular dynamics simulations, and we also observed four possible orientations of **9a** at the agonist-binding site of 5-HT_{1A}R by molecular docking and binding free energy calculations. We found that the tail group of lead compound **9a** can also take different poses at the subsite of 5-HT_{1A}R, namely, the phenyl-up and phenyl-down. Taking advantage of the flip-packing, we virtually designed new **9a** derivatives with different substituents at the headgroup through first-principles calculations and molecular docking operations. These computational designs were validated by our wet-experimental measurements (i.e., chemical synthesis, binding assays, and functional assays) and have led to the discovery of nM-level agonists (e.g., the new compound **9e**). By tuning the binding flexibility of the tail group of lead compound **9a**, we also discovered nM-level 5-HT_{1A}R agonists with the same headgroup of **9a**, e.g., the new compound **9i_2**. The all-in-one tuning on lead compound **9a** has resulted in the discovery of higher-affinity agonists (**9o** and **9p**) of 5-HT_{1A}R, with ~50-fold increase of binding affinity, significantly improved agonistic function (EC_{50}), and also very high 5-HT_{1A}R selectivity. The combinatory approach based on both the computational predicting and wet-experimental validation has been proven to work perfectly in our design of higher-affinity agonists for 5-HT_{1A}R, and thus, this approach can also be generally

applied to design highly active ligands of other subtype 5-HT receptors.

■ ASSOCIATED CONTENT

■ Supporting Information

Four figures, procedures for chemical synthesis, detailed spectral data, coordinates for the modeled 5-HT_{1A}R, and possible orientations for **9e**. The Supporting Information is available free of charge on the ACS Publications website at DOI: 10.1021/acs.jcim.5b00164.

■ AUTHOR INFORMATION

Corresponding Authors

*E-mail: zhenxuechu@suda.edu.cn.

*Fax: +86-21-51980010. Phone: +86-21-51980010. E-mail: wfu@fudan.edu.cn.

Author Contributions

§Peng Lian and LinLang Li contributed equally to this work.

Notes

The authors declare no competing financial interest.

■ ACKNOWLEDGMENTS

This work was supported by the National Natural Science Foundation of China (No. 81172919, 81473136, 81130023, 81373382, 31400624) and National Basic Research Plan (973) of the Ministry of Science and Technology of China (2011CB5C4403). Support from the Priority Academic Program Development of Jiangsu Higher Education Institutes (PAPD) and a grant obtained from the Jiangsu Science and Technology commission (BM2013003) are appreciated.

■ REFERENCES

- (1) Franchini, S.; Prandi, A.; Sorbi, C.; Tait, A.; Baraldi, A.; Angeli, P.; Buccioni, M.; Cilia, A.; Poggesi, E.; Fossa, P.; Brasili, L. Discovery of A New Series of 5-HT_{1A} Receptor Agonists. *Bioorg. Med. Chem. Lett.* **2010**, *20*, 2017–2020.
- (2) Valhondo, M.; Marco, I.; Martín-Fontecha, M.; Vázquez-Villa, H.; Ramos, J. A.; Berkels, R.; Lauterbach, T.; Benhamú, B.; López-Rodríguez, M. L. New Serotonin 5-HT_{1A} Receptor Agonists Endowed with Antinociceptive Activity in Vivo. *J. Med. Chem.* **2013**, *56*, 7851–7861.
- (3) Lacivita, E.; Di Pilato, P.; De Giorgio, P.; Colabufo, N. A.; Berardi, F.; Perrone, R.; Leopoldo, M. The Therapeutic Potential of 5-HT_{1A} Receptors: A Patent Review. *Expert Opin. Ther. Pat.* **2012**, *22*, 887–902.
- (4) Liu, Z.; Zhang, H.; Ye, N.; Zhang, J.; Wu, Q.; Sun, P.; Li, L.; Zhen, X.; Zhang, A. Synthesis of Dihydrofuroaporphine Derivatives: Identification of a Potent and Selective Serotonin 5-HT_{1A} Receptor Agonist. *J. Med. Chem.* **2010**, *53*, 1319–1328.
- (5) Wrobel, M. Z.; Chodkowski, A.; Herold, F.; Gomolka, A.; Kleps, J.; Mazurek, A. P.; Plucinski, F.; Mazurek, A.; Nowak, G.; Siwek, A.; Stachowicz, K.; Slawinska, A.; Wolak, M.; Szewczyk, B.; Satala, G.; Bojarski, A. J.; Turlo, J. Synthesis and Biological Evaluation of Novel Pyrrolidine-2,5-dione Derivatives as Potential Antidepressant Agents. Part 1. *Eur. J. Med. Chem.* **2013**, *63*, 484–500.
- (6) Mueller, C. P.; Carey, R. J.; Huston, J. P.; Silva, M. A. D. S. Serotonin and Psychostimulant Addiction: Focus on 5-HT_{1A}-receptors. *Prog. Neurobiol.* **2007**, *81*, 133–178.
- (7) Lanoir, J.; Hilaire, G.; Seif, I. Reduced Density of Functional 5-HT_{1A} Receptors in the Brain, Medulla and Spinal Cord of Monoamine Oxidase-A Knockout Mouse Neonates. *J. Comp. Neurol.* **2006**, *495*, 607–623.
- (8) Jason Hannon, D. H. Serotonin Receptors and Systems: Endless Diversity. *Acta Biol. (Szeged)* **2002**, *42*, 1–12.
- (9) Weber, K. C.; Salum, L. B.; Honorio, K. M.; Andricopulo, A. D.; da Silva, A. B. Pharmacophore-based 3D QSAR Studies on a Series of High

Affinity 5-HT_{1A} Receptor Ligands. *Eur. J. Med. Chem.* **2010**, *45*, 1508–1514.

(10) Dilly, S.; Graulich, A.; Liegeois, J. F. Molecular Modeling Study of 4-phenylpiperazine and 4-phenyl-1,2,3,6-tetrahydropyridine Derivatives: A New Step Towards the Design of High-affinity 5-HT_{1A} Ligands. *Bioorg. Med. Chem. Lett.* **2010**, *20*, 1118–1123.

(11) Hendry, N.; Christie, I.; Rabiner, E. A.; Laruelle, M.; Watson, J. In vitro Assessment of the Agonist Properties of the Novel 5-HT_{1A} Receptor Ligand, CUMI-101 (MMP), in Rat Brain Tissue. *Nucl. Med. Biol.* **2011**, *38*, 273–277.

(12) Kuipers, W.; Kruse, C. G.; van Wijngaarden, I.; Standaar, P. J.; Tulp, M. T. M.; Veldman, N.; Spek, A. L.; Ijzerman, A. P. 5-HT_{1A}-versus D₂-Receptor Selectivity of Flesinoxan and Analogous N-4-Substituted N-1-Arylpiperazines. *J. Med. Chem.* **1997**, *40*, 300–312.

(13) Vicente, M. A.; Zangrossi, H., Jr.; dos Santos, L.; de Macedo, C. E.; Andrade, T. G. Involvement of Median Raphe Nucleus 5-HT_{1A} Receptors in the Regulation of Generalized Anxiety-related Defensive Behaviours in Rats. *Neurosci. Lett.* **2008**, *445*, 204–208.

(14) Albert, P. R.; Lemonde, S. 5-HT_{1A} Receptors, Gene Repression, and Depression: Guilt by Association. *Neuroscientist* **2004**, *10*, 575–593.

(15) Slowinski, T.; Stefanowicz, J.; Dawidowski, M.; Kleps, J.; Czuczwar, S.; Andres-Mach, M.; Luszczki, J. J.; Nowak, G.; Stachowicz, K.; Szewczyk, B.; Slawinska, A.; Mazurek, A. P.; Mazurek, A.; Plucinski, F.; Wolska, I.; Herold, F. Synthesis and Biological Investigation of Potential Atypical Antipsychotics with a Tropane Core. Part 1. *Eur. J. Med. Chem.* **2011**, *46*, 4474–4488.

(16) Yuan, Q.; Joiner, W. J.; Sehgal, A. A Sleep-promoting Role for the Drosophila Serotonin Receptor 1A. *Curr. Biol.* **2006**, *16*, 1051–1062.

(17) Mo, J.; Zhang, H.; Yu, L.-P.; Sun, P.-H.; Jin, G.-Z.; Zhen, X. 1-Stepholidine Reduced 1-DOPA-induced Dyskinesia in 6-OHDA-lesioned Rat Model of Parkinson's Disease. *Neurobiol. Aging* **2010**, *31*, 926–936.

(18) Zhang, H.; Ye, N.; Zhou, S.; Guo, L.; Zheng, L.; Liu, Z.; Gao, B.; Zhen, X.; Zhang, A. Identification of N-propylnoraporphine-11-yl 5-(1,2-dithiolan-3-yl)pentanoate as a New Anti-Parkinson's Agent Possessing a Dopamine D₂ and Serotonin 5-HT_{1A} Dual-agonist Profile. *J. Med. Chem.* **2011**, *54*, 4324–4338.

(19) Zhao, R.; Lu, W.; Fang, X.; Guo, L.; Yang, Z.; Ye, N.; Zhao, J.; Liu, Z.; Jia, J.; Zheng, L.; Zhao, B.; Zhang, A.; Zhen, X. (6aR)-11-amino-N-propyl-noraporphine, a New Dopamine D₂ and Serotonin 5-HT_{1A} Dual Agonist, Elicits Potent Antiparkinsonian Action and Attenuates Levodopa-induced Dyskinesia in a 6-OHDA-lesioned Rat Model of Parkinson's Disease. *Pharmacol., Biochem. Behav.* **2014**, *124*, 204–210.

(20) Altieri, S. C.; Garcia-Garcia, A. L.; Leonardo, E. D.; Andrews, A. M. Rethinking 5-HT_{1A} Receptors: Emerging Modes of Inhibitory Feedback of Relevance to Emotion-related Behavior. *ACS Chem. Neurosci.* **2013**, *4*, 72–83.

(21) Fox, S. H.; Chuang, R.; Brotchie, J. M. Serotonin and Parkinson's Disease: On Movement, Mood, and Madness. *Mov. Disord.* **2009**, *24*, 1255–1266.

(22) Celada, P.; Bortolozzi, A.; Artigas, F. Serotonin 5-HT_{1A} Receptors as Targets for Agents to Treat Psychiatric Disorders: Rationale and Current Status of Research. *CNS Drugs* **2013**, *27*, 703–716.

(23) Murata, Y.; Yanagihara, Y.; Mori, M.; Mine, K.; Enjoji, M. Chronic Treatment with Tandoospirone, a Serotonin 1A Receptor Partial Agonist, Inhibits Psychosocial Stress-induced Changes in Hippocampal Neurogenesis and Behavior. *J. Affective Disord.* **2015**, *180*, 1–9.

(24) McKean, J.; Watts, H.; Mokszycki, R. Breakthrough Seizures after Starting Vilazodone for Depression. *Pharmacotherapy* **2015**, *35*, E6–E8.

(25) Gommoll, C.; Durgam, S.; Mathews, M.; Forero, G.; Nunez, R.; Tang, X.; Thase, M. E. A Double-blind, Randomized, Placebo-controlled, Fixed-dose Phase III Study of Vilazodone in Patients with Generalized Anxiety Disorder. *Depression Anxiety* **2015**, *32*, 451–459.

(26) Colpaert, F. C.; Tarayre, J. P.; Koek, W.; Pauwels, P. J.; Bardin, L.; Xu, X. J.; Wiesenfeld-Hallin, Z.; Cosi, C.; Carilla-Durand, E.; Assie, M. B.; Vacher, B. Large-amplitude 5-HT_{1A} Receptor Activation: A New Mechanism of Profound, Central Analgesia. *Neuropharmacology* **2002**, *43*, 945–958.

- (27) Guo, Y.; Zhang, H.; Chen, X.; Cai, W.; Cheng, J.; Yang, Y.; Jin, G.; Zhen, X. Evaluation of the Antipsychotic Effect of Bi-acetylated l-stepholidine (l-SPD-A), a Novel Dopamine and Serotonin Receptor Dual Ligand. *Schizophr. Res.* **2009**, *115*, 41–49.
- (28) Xu, L.; Zhou, S.; Yu, K.; Gao, B.; Jiang, H.; Zhen, X.; Fu, W. Molecular Modeling of the 3D Structure of 5-HT(1A)R: Discovery of Novel 5-HT(1A)R Agonists via Dynamic Pharmacophore-based Virtual Screening. *J. Chem. Inf. Model.* **2013**, *53*, 3202–3211.
- (29) Lian, P.; Xu, L.; Geng, C.; Qian, Y.; Li, W.; Zhen, X.; Fu, W. A Computational Perspective on Drug Discovery and Signal Transduction Mechanism of Dopamine and Serotonin Receptors in the Treatment of Schizophrenia. *Curr. Pharm. Biotechnol.* **2014**, *15*, 916–926.
- (30) Bang, I.; Choi, H.-J. Structural Features of β_2 Adrenergic Receptor: Crystal Structures and Beyond. *Mol. Cells* **2015**, *38*, 105–111.
- (31) Lebon, G.; Warne, T.; Edwards, P. C.; Bennett, K.; Langmead, C. J.; Leslie, A. G. W.; Tate, C. G. Agonist-bound Adenosine A(2A) Receptor Structures Reveal Common Features of GPCR Activation. *Nature* **2011**, *474*, 521–525.
- (32) Zhang, J.; Zhang, K.; Gao, Z.-G.; Paoletta, S.; Zhang, D.; Han, G. W.; Li, T.; Ma, L.; Zhang, W.; Mueller, C. E.; Yang, H.; Jiang, H.; Cherezov, V.; Katritch, V.; Jacobson, K. A.; Stevens, R. C.; Wu, B.; Zhao, Q. Agonist-bound Structure of the Human P2Y(12) Receptor. *Nature* **2014**, *509*, 119–122.
- (33) Xu, F.; Wu, H. X.; Katritch, V.; Han, G. W.; Jacobson, K. A.; Gao, Z. G.; Cherezov, V.; Stevens, R. C. Structure of an Agonist-Bound Human A(2A) Adenosine Receptor. *Science* **2011**, *332*, 322–327.
- (34) Kandt, C.; Ash, W. L.; Peter Tieleman, D. Setting up and Running Molecular Dynamics Simulations of Membrane Proteins. *Methods* **2007**, *41*, 475–488.
- (35) Berendsen, H. J. C.; Postma, J. P. M.; van Gunsteren, W. F.; Hermans, J. Interaction Models for Water in Relation to Protein Hydration. In *Intermolecular Forces*, Pullman, B., Ed.; D. Reidel Publishing Company: 1981; pp 331–342.
- (36) Hess, B.; Kutzner, C.; van der Spoel, D.; Lindahl, E. GROMACS 4: Algorithms for Highly Efficient, Load-Balanced, and Scalable Molecular Simulation. *J. Chem. Theory Comput.* **2008**, *4*, 435–447.
- (37) Berger, O.; Edholm, O.; Jähnig, F. Molecular Dynamics Simulations of a Fluid Bilayer of Dipalmitoylphosphatidylcholine at Full Hydration, Constant Pressure, and Constant Temperature. *Biophys. J.* **1997**, *72*, 2002–2013.
- (38) Schüttelkopf, A. W.; van Aalten, D. M. PRODRG: A Tool for High-throughput Crystallography of Protein-ligand Complexes. *Acta Crystallogr., Sect. D: Biol. Crystallogr.* **2004**, *60*, 1355–1363.
- (39) Frisch, M. J.; Trucks, G. W.; Schlegel, H. B.; Scuseria, G. E.; Robb, M. A.; Cheeseman, J. R.; Scalmani, G.; Barone, V.; Mennucci, B.; Petersson, G. A.; Nakatsuji, H.; Caricato, M.; Li, X.; Hratchian, H. P.; Izmaylov, A. F.; Bloino, J.; Zheng, G.; Sonnenberg, J. L.; Hada, M.; Ehara, M.; Toyota, K.; Fukuda, R.; Hasegawa, J.; Ishida, M.; Nakajima, T.; Honda, Y.; Kitao, O.; Nakai, H.; Vreven, T.; Montgomery, J. A., Jr.; Peralta, P. E.; Ogliaro, F.; Bearpark, M.; Heyd, J. J.; Brothers, E.; Kudin, K. N.; Staroverov, V. N.; Kobayashi, R.; Normand, J.; Raghavachari, K.; Rendell, A.; Burant, J. C.; Iyengar, S. S.; Tomasi, J.; Cossi, M.; Rega, N.; Millam, N. J.; Klene, M.; Knox, J. E.; Cross, J. B.; Bakken, V.; Adamo, C.; Jaramillo, J.; Gomperts, R.; Stratmann, R. E.; Yazyev, O.; Austin, A. J.; Cammi, R.; Pomelli, C.; Ochterski, J. W.; Martin, R. L.; Morokuma, K.; Zakrzewski, V. G.; Voth, G. A.; Salvador, P.; Dannenberg, J. J.; Dapprich, S.; Daniels, A. D.; Farkas, Ö.; Ortiz, J. V.; Cioslowski, J.; Fox, D. J. *Gaussian 09*, Gaussian, Inc.: Wallingford, CT, 2009.
- (40) Hoover, W. Canonical Dynamics: Equilibrium Phase-space Distributions. *Phys. Rev. A: At., Mol., Opt. Phys.* **1985**, *31*, 1695–1697.
- (41) Nosé, S. A Molecular Dynamics Method for Simulations in the Canonical Ensemble. *Mol. Phys.* **1984**, *52*, 255–268.
- (42) Nosé, S.; Klein, M. L. Constant Pressure Molecular Dynamics for Molecular Systems. *Mol. Phys.* **1983**, *50*, 1055–1076.
- (43) Parrinello, M.; Rahman, A. Polymorphic Transitions in Single Crystals: A New Molecular Dynamics Method. *J. Appl. Phys.* **1981**, *52*, 7182–7190.
- (44) Hess, B.; Bekker, H.; Berendsen, H. J. C.; Fraaije, J. G. E. M. LINCS: A Linear Constraint Solver for Molecular Simulations. *J. Comput. Chem.* **1997**, *18*, 1463–1472.
- (45) Darden, T.; York, D.; Pedersen, L. Particle Mesh Ewald: An N. log(N) Method for Ewald Sums in Large Systems. *J. Chem. Phys.* **1993**, *98*, 10089–10092.
- (46) Lian, P.; Angela Liu, L.; Shi, Y.; Bu, Y.; Wei, D. Tethered-Hopping Model for Protein-DNA Binding and Unbinding Based on Sox2-Oct1-Hoxb1 Ternary Complex Simulations. *Biophys. J.* **2010**, *98*, 1285–1293.
- (47) Lian, P.; Li, J.; Wang, D. Q.; Wei, D. Q. Car-Parrinello Molecular Dynamics/Molecular Mechanics (CPMD/MM) Simulation Study of Coupling and Uncoupling Mechanisms of Cytochrome P450cam. *J. Phys. Chem. B* **2013**, *117*, 7849–7856.
- (48) Lian, P.; Wei, D.-Q.; Wang, J.-F.; Chou, K.-C. An Allosteric Mechanism Inferred from Molecular Dynamics Simulations on Phospholamban Pentamer in Lipid Membranes. *PLoS One* **2011**, *6*, e18587.
- (49) Lian, P.; Guo, H.-B.; Smith, J. C.; Wei, D.-Q.; Guo, H. Catalytic Mechanism and Origin of High Activity of Cellulase TmCel12A at High Temperature: A Quantum Mechanical/Molecular Mechanical Study. *Cellulose* **2014**, *21*, 937–949.
- (50) Morris, G. M.; Huey, R.; Lindstrom, W.; Sanner, M. F.; Belew, R. K.; Goodsell, D. S.; Olson, A. J. AutoDock4 and AutoDockTools4: Automated Docking with Selective Receptor Flexibility. *J. Comput. Chem.* **2009**, *30*, 2785–2791.
- (51) Sanner, M. F. Python: A programming language for software integration and development. *J. Mol. Graphics Modell.* **1999**, *17*, 57–61.
- (52) *Schrödinger Release 2013-3*, Schrödinger, LLC, New York, 2013.